

Polyanilino-Carbon Nanotubes Derivatized Cytochrome P450 2E1 Nanobiosensor for the Determination of Pyrazinamide Anti- tuberculosis drugs

Unathi Sidwaba¹, Rachel F. Ajayi¹, Usisipho Feleni¹, Samantha Douman¹,
Priscilla G.L. Baker¹, Sibulelo L. Vilakazi², Robert Tshikhudo²,
Emmanuel I. Iwuoha^{1*}

¹SensorLab, Department of Chemistry, University of the Western Cape,
Private Bag X17, Bellville, 7535, South Africa

²Nanotechnology Innovation Centre, Advanced Materials Division,
Mintek, Randburg, Johannesburg, South Africa.

*e-mail: eiwuoha@uwc.ac.za

Keywords: Pyrazinamide, Cytochrome P450-2E1, Cyclic voltammetry, Tuberculosis, Polyaniline, Carbon nanotubes, Atomic Force Microscopy.

Abstract. Pyrazinamine (PZA) is one of the most commonly prescribed anti-tuberculosis (anti-TB) drug due to its ability to significantly shorten the TB treatment period. However, excess PZA in the body causes hepatotoxicity and liver damage. This, therefore, calls for new methods for ensuring reliable dosing of the drug, which will differ from person to person due to interindividual differences in drug metabolism. A novel biosensor system for monitoring the metabolism of PZA was prepared with nanocomposite of multi-walled carbon nanotubes (MWCNTs), polyaniline (PANI) and cytochrome P450 3A4 (CYP3A4) electrochemically deposited on a glassy carbon electrode (GCE). The nanocomposite biosensor system exhibited enhanced electroactivity that is attributable to the catalytic effect of the incorporated MWCNTs. The biosensor had a sensitivity of $7.80 \mu\text{A}/\mu\text{g mL}^{-1}$ PZA and a dynamic linear range of 4.92 – 160 ng/mL PZA.

Introduction

Pyrazinamide (PZA) is one of the first-line drugs in the multi-drug regimen treatment of tuberculosis (TB), which affects one third of the world [1] at a rate of one new infection per second. Pyrazinamide (see structure in Fig. 1) is normally administered along with ethambutol, isoniazid and rifampicin. PZA is the most effective of the four drugs and has been proven to shorten tuberculosis therapy from nine months to the current six months duration [2]. The metabolic clearance of PZA varies from person to person due to the polymorphic behaviour of enzymes, leading to different rates at which the drugs are metabolized. Such variations lead to severe side effects caused by the accumulation of the drug in the human system. The most common side effects of PZA include hepatotoxicity and liver damage, which calls for very sensitive and reliable devices for their monitoring [3].

Electrochemical methods are being developed for fast on-site monitoring of drugs. [4]. Some of these methods involve the use of conductive polymers. This class of polymers have been intensively researched on as platforms for the immobilisation of enzymes during biosensor fabrication. In biosensor systems the polymers act as receptors for biomolecule and mediators for electron transport between the electrode and the active site of the biomolecule [5]. Most common and widely studied polymers include polyaniline, polypyrrole, polyacetylene and polythiophene [6, 7]. Polyaniline (PANI) has attracted much interest among academic and industrial researchers due to its outstanding electrochemical, optical, physical, chemical and mechanical properties; together with its environmental stability and ease of preparation by chemical or electrochemical procedures [8-10]. Though PANI has applications in sensors, electronics devices and batteries, it is normally conductive in acidic mediums, which limits its application [11]. The modification or tuning of the conductivity properties of PANI can be effected with nanomaterials, transition metal oxides and organic dopants [12].

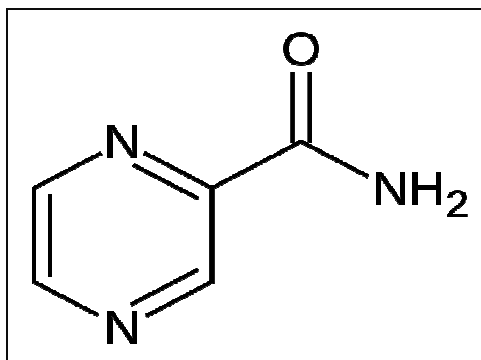


Fig. 1. Structure of pyrazinamide.

Carbon nanotubes (CNTs) have been intensively applied the development of biosensors due to their unique structural, electronic and mechanical properties [13]. They are characterised by large surface area and high conductivity which result in enhanced performance of CNT nanocomposites with other materials. Several studies have also demonstrated that CNTs enhance the electrochemical reactivity of immobilized biomolecules by promoting faster electron transfer reactions [14]. In this study a multi-walled carbon nanotube (MWCNT) has been combined with PANI to produce a biocompatible platform for the immobilisation of cytochrome P450 3A4 (CYP3A4) for the preparation of a novel nanobiosensor system for the determination of PZA.

Experimental

Reagents. Aniline (93.13%) was purchased from Sigma Aldrich, South Africa and was purified by vacuum distillation. Carboxylic acid functionalized carbon nanotubes, sodium dihydrogen phosphate monobasic anhydrous (NaH_2PO_4) and disodium phosphate dibasic dihydrate ($\text{Na}_2\text{PO}_4 \cdot 2\text{H}_2\text{O}$), hydrochloric acid (HCl), MWCNTs and absolute ethanol were also purchased from Sigma-Aldrich and used without further purification. NaH_2PO_4 and $\text{Na}_2\text{PO}_4 \cdot 2\text{H}_2\text{O}$ were used in the preparation of 0.1 M phosphate buffer solution pH 7.4 (PBS). Pyrazinamide drug was obtained from University of Western Cape Health Centre as a tablet formulation containing 500 mg pyrazinamide. A stock solution of 8.20 μM cytochrome P450 2E1 enzyme (EC 1.14.14.1) was supplied by Sigma Aldrich. De-ionized water, used for all experiments, was prepared with a Milli-Q water purification system. Analytical grade argon obtained from Afrox South Africa was used for degassing the cell solutions.

Instrumentation. All electrochemical experiments were carried out with a BioAnalytical Systems (BAS) 100W electrochemical workstation; and a three electrode cell system with a BAS 0.071 cm² glassy carbon electrode (GCE), a Sigma Aldrich platinum wire and a BAS Ag/AgCl (3 M NaCl type) as the working, counter and reference electrodes, respectively. Prior to use, the GCE was polished with 1.0, 0.3 and 0.05 μm alumina slurries (Buehler, IL, USA), followed by ultrasonication in absolute ethanol and deionised water.

Preparation of GCE/PANI/MWCNT/CYP2E1 Nanobiosensor. The polymerisation monomer was prepared by refluxing a 0.1 M aniline solution containing 0.2 % wt MWCNT at 130 °C for 3 h and followed by vacuum filtration. The PANI-MWCNT film was deposited on GCE by oxidative electropolymerization of the aniline-MWCNT solution by scanning the electrode at 40 mV/s from -250 mV to +950 mV for 10 cycles. The PANI-MWCNT polymer film was reduced at -500 mV for 1200 s. The reduced polymer film was then immersed in a PBS cell solution containing 20 μL of CYP2E1. The modified electrode was then oxidised at +400 mV for 1800 s, during which CYP2E1 was deposited on the PANI-MWCNT film by chemical and electrostatic interactions as depicted in Fig 2. The biosensor (denoted as GCE/PANI/MWCNT/CYP2E1) was carefully rinsed with water and stored at 4 °C when not in use.

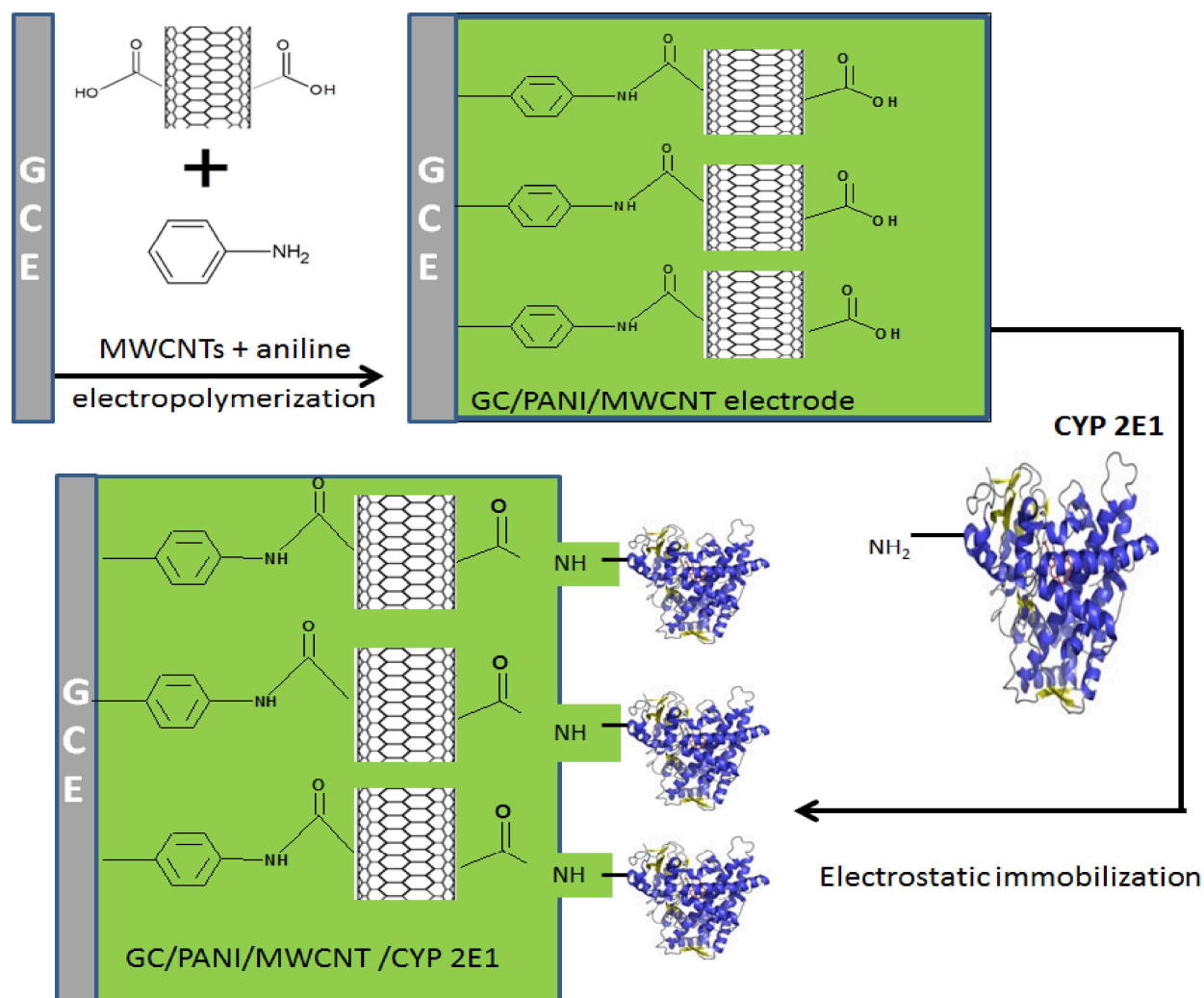


Fig. 2. Schematic representation of the preparation of the nanobiosensor.

Results and Discussion

Morphology of PANI-MWCNT. The AFM pictures of PANI-MWCNT nanocomposite and its components are in Fig. 3. The PANI-MWCNT nanocomposite exhibits tubular structures (Fig. 3C), while PANI (Fig. 3B) displays small spherical particles of uniform size. When MWCNTs were incorporated into PANI, the resultant PANI-MWCNT nanocomposite has a different AFM morphology that reveals the distribution of MWCNTs (of 115 nm average diameter) within the composite.

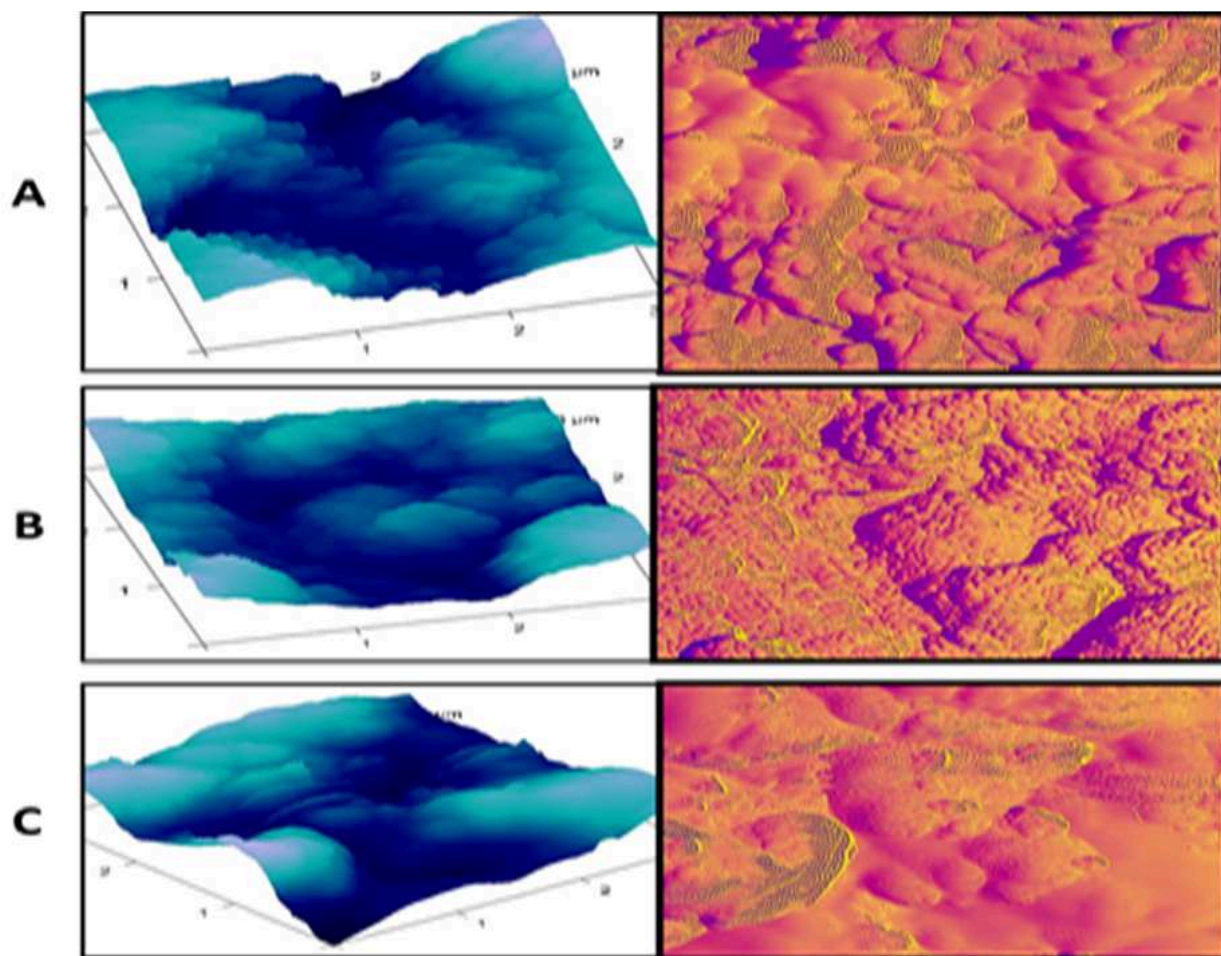


Fig. 3. AFM images of MWCNTs (A), PANI (B) and PANI-MWCNT composite (C).

The XRD patterns in Fig. 4 consist of sharp well-resolved peaks at 26.0° and 26.5° associated with carbon (002) in MWCNTs [15, 16] and PANI [17], respectively. The distinctive sharpness of the peaks is indicative of the crystallinity of both MWCNTs and PANI [17]. However, in the nanocomposite (MWCNT-PANI) the characteristic XRD peak value shifted to 25.8° due to the bonding between PANI and MWCNTs.

Electrochemical Properties. The nanocomposite was characterized using cyclic voltammetry (CV) and differential pulse voltammetry (DPV). The CV graphs (Fig. 5A) have three redox processes corresponding to A/A' (+ 260/+210 mV), B/B' (+480/+560 mV) and C/C' (+590/+620 mV) at lower scan rates. The redox process A/A', B/B' and C/C' can be attributed to the leucoemeraldine/leucoemeraldine radical cation, emeraldine radical cation/emeraldine and

pernigraniline radical cation/pernigraniline states of PANI, respectively [18, 19]. At higher scan rates, there are two redox pairs with peak C broadening out and disappearing at scan rates of 50 to 60 mV s^{-1} . It can therefore be concluded that the rate at which the pernigraniline radical cation gains an electron is very slow. The voltammograms correspond to a reversible system with $I_{p,a}(\text{peak A})/I_{p,c}(\text{peak A}')$ value of 1.2 and $\Delta E_p = E_{p,a}(\text{peak A}) - E_{p,c}(\text{peak A}') < 57/n \text{ mV}$. These are characteristic of a surface adsorbed species undergoing fast reversible electron transfer reaction [18]. There is a distinct increase in the current density with increasing scan rates between the scan rates of 10 and 60 mV/s . There is also an observed shift in the peak potential for redox pairs A/A' and C/C' which is indicative of electron hopping along the polymer chain [20].

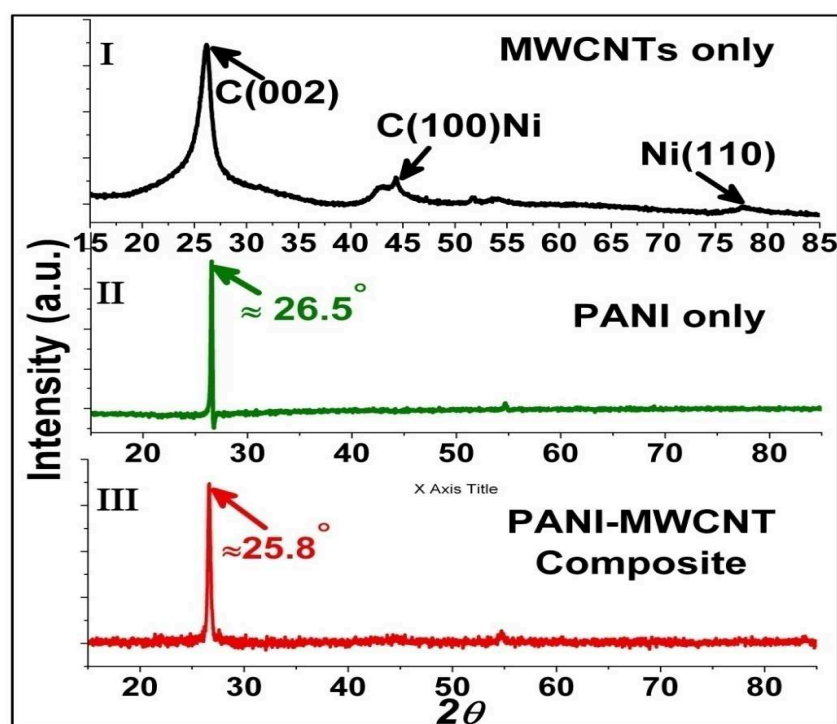


Fig. 4. X-ray diffractogram of MWCNTs, PANI and PANI-MWCNT composite.

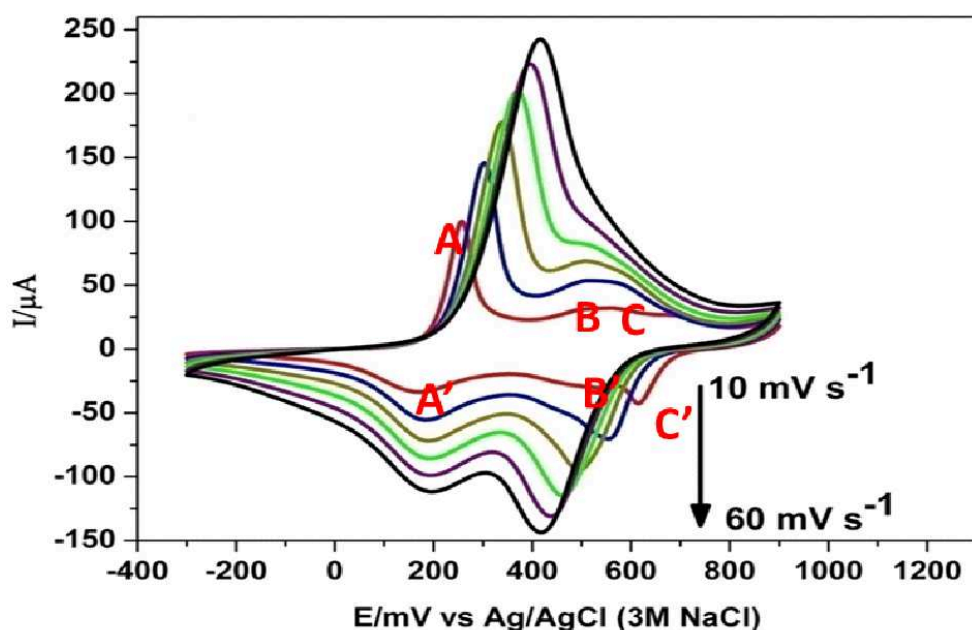


Fig. 5. Cyclic voltammograms of GCE/PANI/MWCNT in 0.1 M PBS, for scan rates of 10 –60 mV s^{-1} at 10 mV s^{-1} intervals.

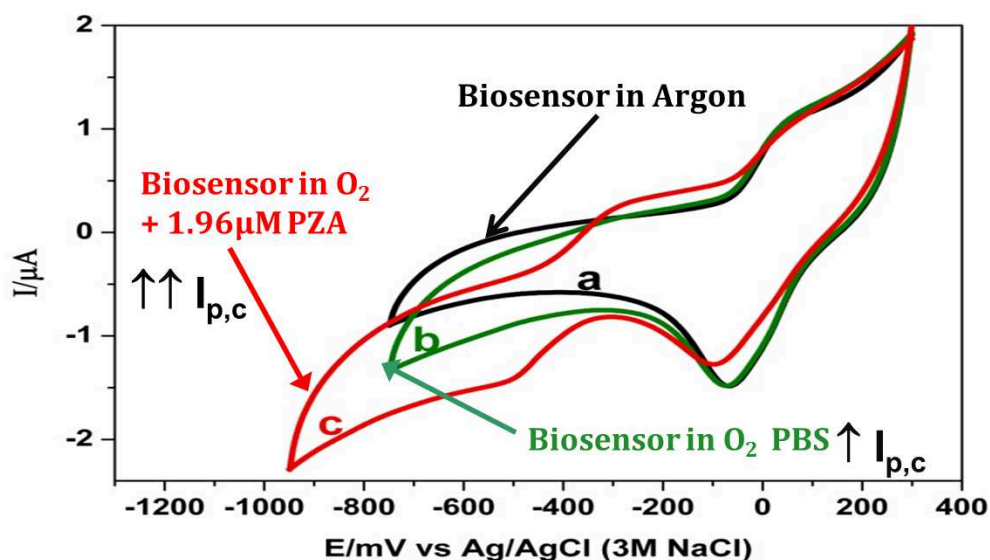


Fig. 6. CV graphs of GCE/PANI/MWCNT/CYP2E1 for different systems.

Response Dynamics of PZA Nanobiosensor. The electrocatalytic behaviour of the biosensor was investigated in the presence and absence of PZA as shown in Fig. 6. The necessity of oxygen during the enzymatic reaction was also investigated. In the presence of oxygen, there was an increase in the cathodic peak current with an onset potential of -160 mV which is indicative of the oxygenation of

CYP2EI heme Fe atom being coupled to the electron transfer reaction that occurs in argon degassed medium represented by voltammogram 'a'. Then, in the presence of 1.96 μM PZA, there was a development of a large cathodic catalytic wave with a peak at -490 mV.

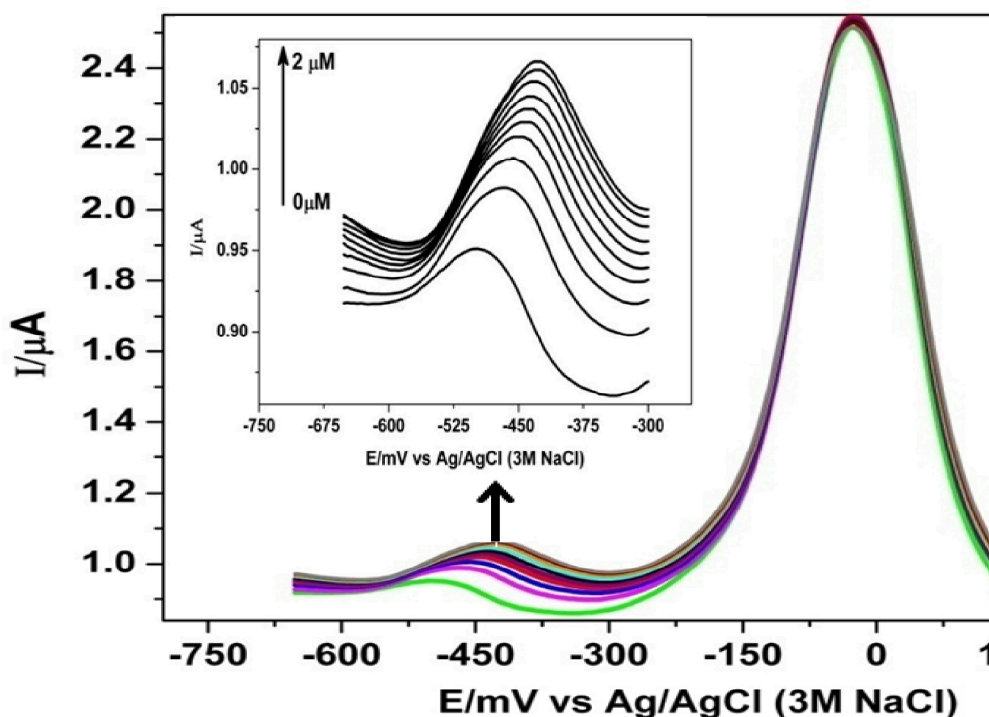


Fig. 7. SWV graphs of GCE/PANI/MWCNT/CYP2E1 for 0 – 2 μM PZA at 0.2 μM increments.

Inset is an expansion of SWVs for -650 to +300 mV.

This behaviour was only observed for the biosensor in the presence of PZA. Voltammogram 'c' consists of a shift of the electron transfer cathodic peak potential (E_{pc}) from -25 mV in argon medium to -50 mV in oxygenated PZA solution. This implies that the electron transfer at the GCE/PANI/MWCNT/CYP2E1 electrode that occurred at -25 mV was followed by (i) the binding of PZA to CYP2EI that shifts the E_{pc} to -50 mV, (ii) the oxygenation (binding of O_2) of PZA-CYP2EI at -160 mV and (ii) the reduction of PZA-CYP2EI- O_2 starting at an onset potential of -300 mV reaching a peak at -490 mV. This result is in agreement with the mechanism for the metabolic reaction of cytochrome P450 (heamolytic) enzymes [21-23]. Figure 6 is the plot of the square wave voltammograms (SWVs) of the biosensor responses to PZA. After the first addition, a catalytic current response resulting from the reduction of PZA was observed at -460 mV. The reduction peak

current increased with increasing concentrations of PZA. This behaviour is attributed to the coupling of the fast electron transfer at the electrode surface with the reduction of PZA on or within the biosensor film [12]. The increase in current is proportional to the amount of the analyte. There was also an observed anodic shift in the peak potential, which is attributed [21-23] to the ease of reduction of the CYP2E1 heme Fe from Fe^{3+} to Fe^{2+} , brought about by the PZA-induced conversion of low spin Fe^{3+} to high spin Fe^{3+} (the later being easier to reduce to Fe^{2+} that preferentially binds O_2).

The peak currents calculated from the SWVs of Fig. 7 inset have a linear relationship with PZA concentrations (see Fig. 8), within a dynamic linear range (DLR) of 0.04 - 1.30 μM PZA (i.e. 4.92 – 160 ng/mL PZA). The sensitivity of the nanobiosensor is 0.96 $\mu\text{A}/\mu\text{M}$ PZA (i.e. 7.80 $\mu\text{A}/\mu\text{g mL}^{-1}$ PZA). The LOD of 500 mg formulation of PZA analysed by liquid chromatography (LC) is 40 ng/mL [24]. This falls within the DLR of the GCE/PANI/MWCNT/CYP2E1 nanobiosensor. However, from LC analysis of human blood [25] the peak concentration (C_{max}) of PZA determined 2 h after drug intake is 3.44 – 4.09 $\mu\text{g/mL}$, which is very detectable with the nanobiosensor due to its high sensitivity (current).

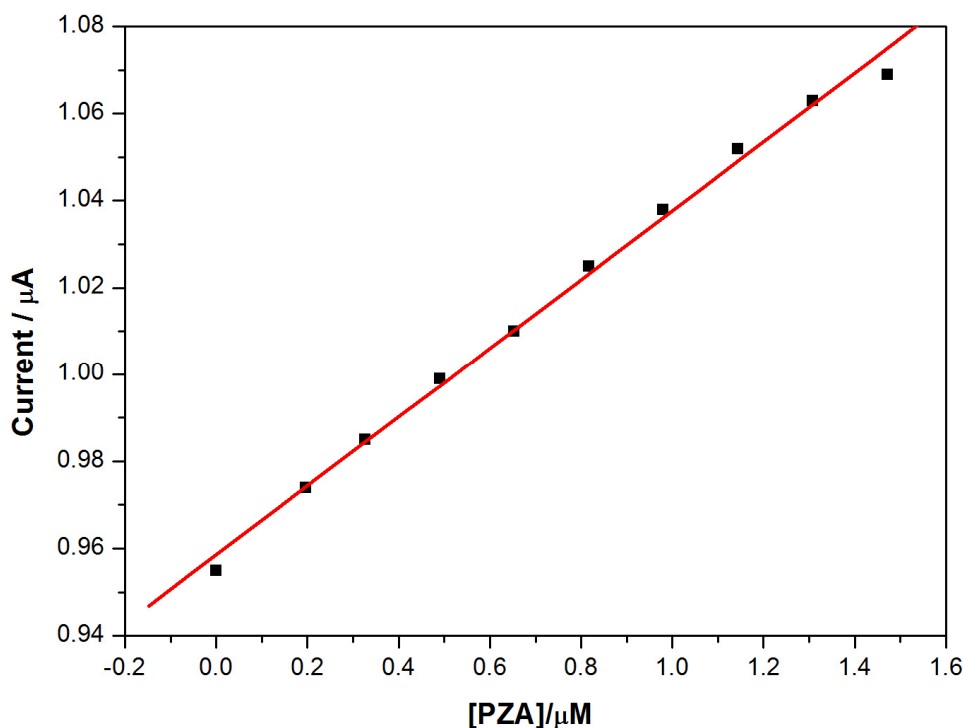


Fig. 8. Calibration plot for PZA nanobiosensor.

Conclusion

The CV results demonstrate that the biosensing process occurs via an oxygenation reaction which culminates in the enzymatic hydroxylation of pyrazinamide to pyrazinoic acid. The reaction is a net 2-electron reduction process in which the first electron is used to reduce Fe^{3+} of CYP2E1 to Fe^{2+} , and the second electron is for splitting the O-O bond of the PZA-CYP2E1- O_2 intermediate [26, 27]. The sensitivity of the biosensor is very much enhanced by the incorporation of MWCNTs into the MWCNT-PANI nanocomposite platform used in the construction of the nanobiosensor. The C_{max} for 500 mg PZA administered to TB patients in Cape Town area of South Africa is $1.47 \mu\text{g/mL}$ [25]. This level of PZA can be determined by the PZA nanobiosensor. Also the DLR of the biosensor can be extended to cover higher concentrations by increasing the PANI-MWCNT film thickness during electropolymerisation and enzyme incorporation steps. Considering that PZA causes liver damage in combination with the occurrence of inter-individual variability in drug metabolic ability due to genetic polymorphism, the determination of very low levels of PZA (with GC/MWCNT/PANI/CYP2E1 nanobiosensor) in biopsy samples of various biological organs will be essential in controlling drug dosage.

Acknowledgements

The study was partially funded by grant and bursaries from the Centre for Scientific and Industrial Research (CSIR), Medical Research Council (MRC), National Research Foundation (NRF) and the Mintek's Nanotechnology Innovation Centre (NIC) of South Africa.

References

- [1] J. van den Boogaard, G.S. Kibiki, E.R. Kisanga, M.J. Boerre, R.E. Aarnoutse, New drugs against tuberculosis: problems, progress, and evaluation of agents in clinical development, *Antimicrob. Agents Chemother.* 53 (2010) 849-862.
- [2] T. Gumbo, C.S.W. Siyambalapitiyage Dona, C. Meek, R. Leff, Pharmacokinetics-pharmacodynamics of pyrazinamide in a novel in vitro model of tuberculosis for sterilizing effect: a paradigm for faster assessment of new antituberculosis drugs, *Antimicrob. Agents Chemother.* 53 (2009) 3197-3204.
- [3] Y.L. Janin, Antituberculosis drugs: ten years of research, *Bioorg. Med. Chem.* 15 (2007) 2479-2513.
- [4] F. Faridbod, M.R. Ganjali, E. Nasli-Esfahani, B. Larijani, S. Riahi, P. Norouz, Potentiometric sensor for quantitative analysis of pioglitazone hydrochloride in tablets based on theoretical studies, *Int. J. Electrochem. Sci.* 5 (2010) 880-894.
- [5] K. Grennan, A.J. Killard, C.J. Hanson. Optimisation and characterisation of biosensors based on polyaniline, *Talanta* 68 (2006) 1591-1600.
- [6] N. Gospodinova, L. Terlemezyan. Conductive Polymers Prepared by Oxidative Polymerization: Polyaniline, *Prog. Polym. Sci.* 23 (1999) 1443-1484.
- [7] M. Matsuguchi, A. Okamoto, Y. Sakai. Effect of humidity on NH₃ gas sensitivity of polyaniline blend films, *Sens. Actuators, B* 94 (2003) 46-52.
- [8] L. Zhang, P. Liu, Synthesis of hollow polyaniline nanoparticles with reactive template, *Mater. Lett.* 64 (2010) 1755-1757.
- [9] M.D. Bedre, R. Deshpande, B. Salimath, V. Abbaraju, Preparation and characterization of polyaniline-CO₃O₄ nanocomposites via interfacial polymerization, *Am. J. M. Sci.* 2 (2012) 39-43.

-
- [10] Drelinkiewicz, M. Hasik, M. Choczyn'ski, Preparation and properties of polyaniline containing palladium, *Mater. Res. Bull.* 33 (1998) 739-762.
- [11] T.H. Le, N.T. Trinh, L.H. Nguyen, H.B. Nguyen, V.A. Nguyen, D.L. Tran, T.D. Nguyen, Electrosynthesis of polyaniline–mutliwalled carbon nanotube nanocomposite films in the presence of sodium dodecyl sulfate for glucose biosensing, *Adv. Nat. Sci. Nanosci. Nanotechnol.* 4 (2013) 025014-025019.
- [12] E.I. Iwuoha, D. Saenz de Villaverde, N.P. Garcia, M.R. Smyth, J.M. Pingarron, Reactivities of organic phase biosensors. 2. The amperometric behaviour of horseradish peroxidase immobilised on a platinum electrode modified with an electrosynthetic polyaniline film, *Biosens. Bioelectron.* 12 (1997) 747-761.
- [13] W. Li, Y. Zheng, X. Fu, J. Peng, L. Ren, P. Wang, W. Song, Electrochemical characterization of multi-walled carbon nanotubes/polyvinyl alcohol coated electrodes for biological applications, *Int. J. Electrochem. Sci.* 8 (2013) 5738-5754.
- [14] W. Wang, J. Chen. Tuberculosis of the head and neck: a review of 20 cases, *Oral Surg. Oral Med. Oral Pathol. Oral Radiol. Endod.* 107 (2009) 381-382.
- [15] Liu, K. Sun, J. Yang, D. Zhao, Toxicological effects of multi-wall carbon nanotubes in rats, *J. Nanopart. Res.* 10 (2008) 1303-1307.
- [16] L. Ji, L. Zhou, X. Bai, Y. Shao, G. Zhao, Y. Qu, C. Wang, Y. Li, Facile synthesis of multiwall carbon nanotubes/iron oxides for removal oftetrabromobisphenol A and Pb(II), *J. Mater. Chem.* 22 (2012) 15853-15862.
- [17] S.B. Kondawar, M.D. Deshpande, S.P. Agrawal, Transport properties of conductive polyaniline nanocomposites based on carbon nanotubes, *International Journal of Composite Materials* 2 (2012) 32-36.

-
- [18] K.M. Molapo, P.M. Ndagili, R.F. Ajayi, G. Mbambisa, S.M. Mailu, N. Njomo, M. Masikini, Electronics of conjugated polymers (I): polyaniline, *Int. J. Electrochem. Sci.* 7 (2012) 11859-11875.
- [19] E. Iwuoha, S.E. Mavundla, V.S. Somerset, L.F. Petrik, M.J. Klink, M. Sekota, P. Baker, Electrochemical and spectroscopic properties of fly ash- polyaniline matrix nanorod composite, *Microchim. Acta* 155 (2006) 453-458.
- [20] M. Muchindu, E. Iwuoha, E. Pool, N. West, N. Jahed, P. Baker, T. Waryo, A. Williams, Electrochemical ochratoxin A immunosensor system developed on sulphonated polyaniline, *Electroanalysis* 23 (2011) 122-128.
- [21] T. Mulaudzi, N. Ludidi, O. Ruzvidzo, M. Morse, N. Hendricks, E. Iwuoha, C. Gehring, Identification of a novel *Arabidopsis thaliana* nitric oxide-binding molecule with guanylate cyclase activity in vitro. *FEBS Lett.* 585 (2011) 2693-2697.
- [22] E.I. Iwuoha, M.R. Smyth, Reactivities of organic phase biosensors: 6. square-wave and differential pulse studies of genetically engineered cytochrome P450cam (CYP101) bioelectrodes in selected solvents. *Biosens. Bioelectron.* 18 (2003) 237-244.
- [23] E. Iwuoha, F. Ngece, M. Klink, P. Baker, Amperometric responses of CYP2D6 drug metabolism nanobiosensor for sertraline: a selective serotonin reuptake inhibitor. *IET Nanobiotechnol.* 1 (2007) 62-67.
- [24] M.Y. Khuhawar, F.M. Rind, Liquid chromatographic determination of isoniazid, pyrazinamide and rifampicin from pharmaceutical preparations and blood, *J. Chromatogr. B* 766 (2002) 357-63.
- [25] H. McIlleron, P. Wash, A. Burger, J. Norman, P.I. Folb, P. Smith, Determinants of rifampin, isoniazid, pyrazinamide and ethambutol pharmacokinetics in a cohort of tuberculosis patients, *Antimicrob. Agents Chemother.* 50 (2006) 1170-1177.

-
- [26] E. Nxusani, P.M. Ndangili, R.A. Olowu, A.N. Jijana, T. Waryo, N. Jahed, R.F. Ajayi, P. Baker, E. Iwuoha, 3-Mercaptopropionic acid capped Ga_2Se_3 nanocrystal-CYP3A4 biosensor for the determination of 17- α -ethinyl estradiol in water, *Nano Hybrids* 1 (2012) 1-22.
- [27] P.N. Ndangili, A.M. Jijana, P.G.L. Baker, E.I. Iwuoha, 3-Mercaptopropionic acid capped ZnSe quantum dot-cytochrome P450 3A4 enzyme biotransducer for 17 beta-estradiol. *J. Electroanal. Chem.* 653(1-2) (2011) 67-74.